Picosecond Pulse Radiolysis of Direct and Indirect Radiolytic Effects in Highly Concentrated Halide Aqueous Solutions

ARTICLE *in* THE JOURNAL OF PHYSICAL CHEMISTRY A · AUGUST 2011

Impact Factor: 2.69 · DOI: 10.1021/jp203609e · Source: PubMed

6 AUTHORS, INCLUDING:

Anna Balcerzyk
Université Paris-Sud 11
8 PUBLICATIONS **61** CITATIONS
SEE PROFILE

Uli Schmidhammer
Université Paris-Sud 11
54 PUBLICATIONS **516** CITATIONS
SEE PROFILE

Jean-Philippe Larbre
Université Paris-Sud 11
11 PUBLICATIONS **242** CITATIONS
SEE PROFILE

Mehran Mostafavi
Université Paris-Sud 11
162 PUBLICATIONS **2,905** CITATIONS
SEE PROFILE

THE JOURNAL OF PHYSICAL CHEMISTRY A

ARTICLE

pubs.acs.org/JPCA

Picosecond Pulse Radiolysis of Direct and Indirect Radiolytic Effects in Highly Concentrated Halide Aqueous Solutions

Anna Balcerzyk, Uli Schmidhammer, Abdel Karim El Omar, Pierre Jeunesse, Jean-Philippe Larbre, and Mehran Mostafavi*

Laboratoire de Chimie Physique, UMR 8000, CNRS/Université Paris-Sud 11, France

Faculté des Sciences d'Orsay, Bât. 349, 91405 Orsay Cedex, France

ABSTRACT: Recently we measured the amount of the single product, Br_3^-, of steady-state radiolysis of highly concentrated Br^- aqueous solutions, and we showed the effect of the direct ionization of Br^- on the yield of Br_3^-. Here, we report the first picosecond pulse-probe radiolysis measurements of ionization of highly concentrated Br^- and Cl^- aqueous solutions to describe the oxidation mechanism of the halide anions. The transient absorption spectra are reported from 350 to 750 nm on the picosecond range for halide solutions at different concentrations. In the highly concentrated halide solutions, we observed that, due to the presence of Na^+, the absorption band of the solvated electron is shifted to shorter wavelengths, but its decay, taking place during the spur reactions, is not affected within the first 4 ns. The kinetic measurements in the UV reveal the direct ionization of halide ions. The analysis of pulse-probe measurements show that after the electron pulse, the main reactions in solutions containing 1 M of Cl^- and 2 M of Br^- are the formation of $ClOH^{-\bullet}$ and $BrOH^{-\bullet}$, respectively. In contrast, in highly concentrated halide solutions, containing 5 M of Cl^- and 6 M of Br^-, mainly $Cl_2^{-\bullet}$ and $Br_2^{-\bullet}$ are formed within the electron pulse without formation of $ClOH^{-\bullet}$ and $BrOH^{-\bullet}$. The results suggest that, not only Br^- and Cl^- are directly ionized into $Br^\bullet$ and $Cl^\bullet$ by the electron pulse, the halide atoms can also be rapidly generated through the reactions initiated by excitation and ionization of water, such as the prompt oxidation by the hole, $H_2O^{+\bullet}$, generated in the coordination sphere of the anion.

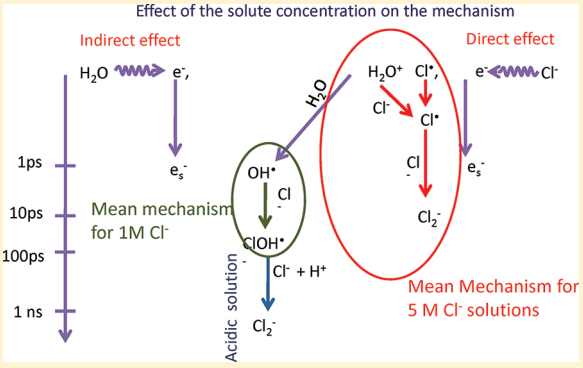

INTRODUCTION

The decomposition of pure water and low concentrated aqueous solutions under irradiation has been studied for 50 years, motivated by various applications in chemistry and biology.[1,2] The radiolytic yields of different species are now well established at the end of the nonhomogenous stage, around 100 ns after energy deposition in the solution.[3,4] Great progress has also been made during the past decade to determine the yield of the hydrated electron back to the picosecond range.[5,6] In contrast, the radiolytic yield of the $OH^\bullet$ radical on the picosecond range is still under discussion due to the experimental problems detecting its low absorption in the middle UV.[3] Usually, indirect scavenging methods are used to determine its radiolytic yield on the different time scales. To obtain data at ultrashort times, the concentration of the scavenger must be very high,[7,8] therefore, the direct ionization of the solute molecules or ions must be considered. Although the radiolysis of pure water or low concentrated aqueous solutions is well-known, this so-called direct effect of ionizing radiation at high solute concentrations is not quantitatively well established.[9] Besides these fundamental questions on radiation chemistry, the direct effect is also important for practical demands in nuclear energy technology as well as for radiotherapy.[1]

Sauer and co-workers studied in detail the electron photodetachment from halide anions in aqueous solutions and determined the ionic strength effect on geminate recombination dynamics and the quantum yield for hydrated electron formation.[10] They showed that, due to the change of the CTTS (charge transfer to the solvent) absorption spectra, the effect of concentration is very important on the photoionization yield of halide anions. But only a few studies have been performed to quantitatively estimate the direct effect of ionizing radiation on the solutes, and their conclusions were not always consistent. In the first instance, the examination of the direct effect was based on highly concentrated nitric acid, which is used in reprocessing of nuclear spent fuels.[11−16] Pulse radiolysis on the nanosecond range revealed that the direct effect leads to the formation of the $NO_3^\bullet$ radical. There are several conflicting results on the direct effect on halide solutions; actually the conclusion is that the yield of the direct effect in aqueous solutions of Cl^- and I^- is around 7×10^{-7} and 7.3×10^{-7} mol J^{-1}, respectively.[17−20] One of the main problems of these reported studies is that the radical yields of water on the picosecond range were not as precisely determined as they are today. There was also some confusion between the scavenging power and the direct effect. Here, highly concentrated bromide

Received: April 18, 2011
Revised: July 19, 2011
Published: July 19, 2011

Table 1. Chemical Composition of Aqueous Solutions Studies by Picosecond Pulse Radiolysis

sample	composition	F	f_s	f_w
1	2 M NaBr	1.1	0.15	0.85
2	6 M NaBr	1.3	0.38	0.62
3	1 M NaCl	1.03	0.05	0.95
4	5 M NaCl	1.13	0.23	0.77
5	1 M NaCl and 1 M $HClO_4$	1.03	0.05	0.95

solutions are proposed as appropriate candidates for measuring the direct radiolytic effect.

Recently, we reported γ-radiolysis studies on highly concentrated aqueous solutions of bromide to examine the total radical yield.[21,22] Bromide concentrations were varied up to 6 M at which almost all $OH^\bullet$ radicals, $H^\bullet$ atoms, and hydrated electrons initially produced react with the bromide anion to ultimately form Br_3^-, a stable species that can be easily measured with a steady state UV−Vis spectrometer. The absorption of the irradiation dose by the solute at high concentration was discussed and quantitatively evaluated. For a concentration of 6 M Br^-, it was found that around 40% of the dose is absorbed by solutes and Br^- is directly ionized.

The precursors of Br_3^- are $BrOH^{-\bullet}$ and $Br_2^{-\bullet}$; both of these species as well as $ClOH^{-\bullet}$ and $Cl_2^{-\bullet}$ present absorption bands with a significant extinction coefficient in the near UV. In the present work, we present picosecond pulse-probe radiolysis measurements to depict the mechanism of halide oxidation by observing these transient species induced by the ultrashort electron pulse. Aqueous solutions with different molar concentrations of NaBr and NaCl are examined to distinguish the direct radiation effect and the initial fundamental radiolytic reaction mechanism.

EXPERIMENTAL SECTION

The chemical reagents were purchased from Sigma-Aldrich. The purity of NaBr and NaCl was greater than 99.9%. Water was purified by passage through a Millipore purification system. The solutions were air saturated and they were prepared at pH 6 as well as at pH 1. The pH of the solutions was adjusted with $HClO_4$. Salt solutions were investigated at 2 and 6 M NaBr and 1 and 5 M NaCl.

The ultrafast pulse radiolysis experiments were performed with a broadband pulse-probe setup that was installed on the experimental area EA-1 of the picosecond electron pulse facility ELYSE. The electron accelerator based on the radiofrequency photogun technology is described in detail elsewhere.[23,24] For the present experiments ELYSE was tuned to deliver electron pulses with energy of 7.1 MeV and a charge of around 4 nC. Recently, single shot electro-optic sampling[25] of the electric field copropagating with the relativistic electron bunch confirmed that ELYSE provides in this configuration electron bunches with a typical pulse duration around 10 ps and a rms shot-to-shot jitter <1 ps.[26] The measurements were performed at the repetition rate of the accelerator set to 10 Hz.

The transient absorption pulse-probe setup is based on the laser-electron intrinsic synchronization resulting from the laser-triggered photocathode[27] and was detailed elsewhere.[28,29] Shortly, the main part of a femtosecond Ti:Sapphire laser output is frequency tripled and used to produce the electron pulse that is accelerated by the RF fields. A part of the laser source is split off to generate the optical probe pulse that can be delayed relative to

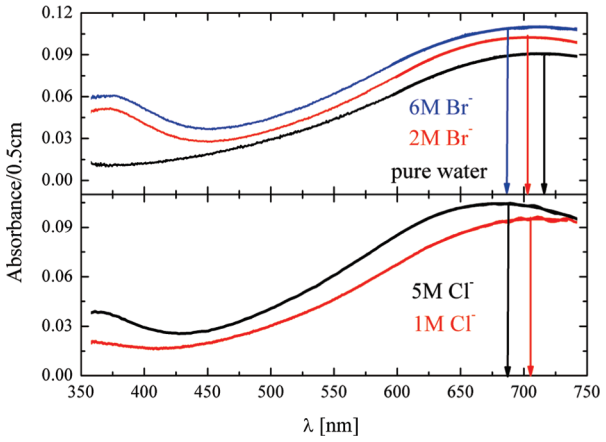

Figure 1. Transient absorption spectra recorded directly after the picosecond electron pulse within a time range of 1 ns. (Top) aqueous solutions of 2 and 6 M NaBr and pure water; (Bottom) 1 and 5 M NaCl.

the electron bunch by a mechanical translation stage. In the present work, about 1 μJ of the laser source was focused into a 6 mm thick CaF_2 disk to generate a supercontinuum whose contribution covering the near UV and visible part was used as optical probe. The intense region around the fundamental laser wavelength at 780 nm was blocked by a combination of KG filters and a solution of a near-infrared laser dye. The probe beam was slightly focused into the sample volume that was irradiated by the electron beam with a diameter of 3−4 mm. A reference signal is split off from the broadband probe before the flow cell. Probe and reference beam were each coupled into an optical fiber, transmitted to a spectrometer and dispersed onto a CCD. The combination of the broadband probe and the multichannel detector allows recording directly entire transient spectra, independently of the shot-to-shot fluctuations and possible long-term drifts of the electron source. For the present work, it is crucial to record simultaneously the transient absorption of the radicals absorbing in the UV and the absorption of the solvated electron in the visible. The latter is used as the reference for the absorbed dose.

All the measurements were made in a flow cell with a 5 mm optical path collinear to the electron pulse propagation. Under the experimental conditions, the time resolution is mainly determined by the electron pulse duration and the velocity mismatch between the electron pulse and the slower visible probe pulse during their propagation inside the cell. Fitting the rise of the absorption signal of the solvated electron, a species that is formed on the femtosecond scale, by a step function convoluted with a Gaussian cross-correlation revealed an apparatus function of full width at half-maximum of 18 ps. More details on the optical configuration and the data acquisition can be found in ref 29.

The solutions containing halide anions at high concentration and pure water were studied under identical experimental conditions. Particular attention was paid for a constant dose per pulse. Transient spectra were recorded on the pico- to low nanosecond scale, the kinetics were traced after data acquisition at selected wavelengths. The temporal evolution of each sample under investigation was scanned in the order of 10 times with a single point averaging of 5−20 for each delay step. The measurements were performed at 22.5 °C, the room temperature during the ps pulse radiolysis experiments.

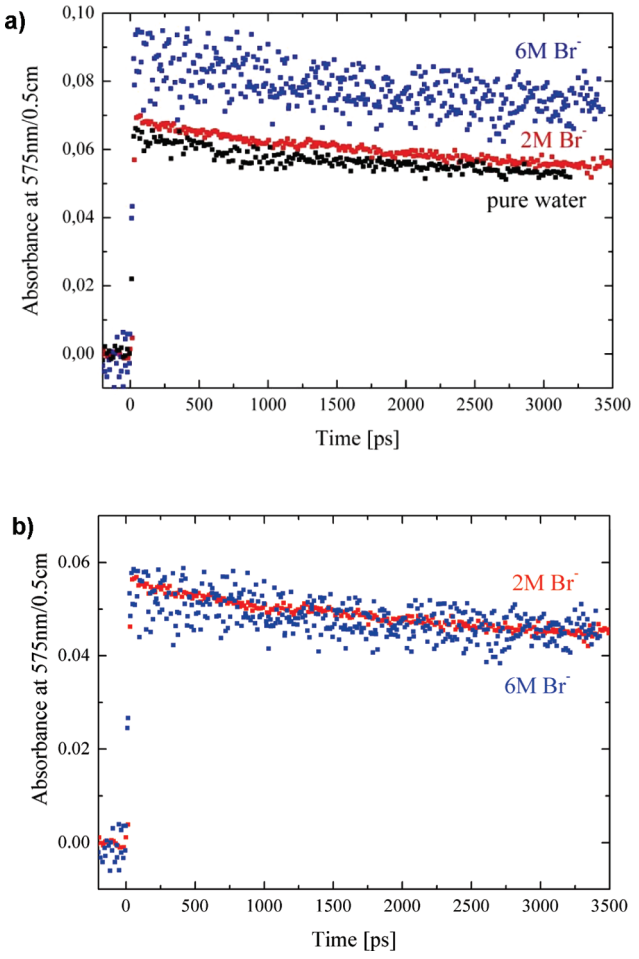

Figure 2. (a) Decay of the solvated electron recorded at 575 nm in aqueous solution of 2 and 6 M NaBr and in pure water without any normalization. (b) Solvated electron decay recorded at 575 nm in aqueous solution of 2 and 6 M NaBr after normalization of the absorbed radiation dose (for details see text).

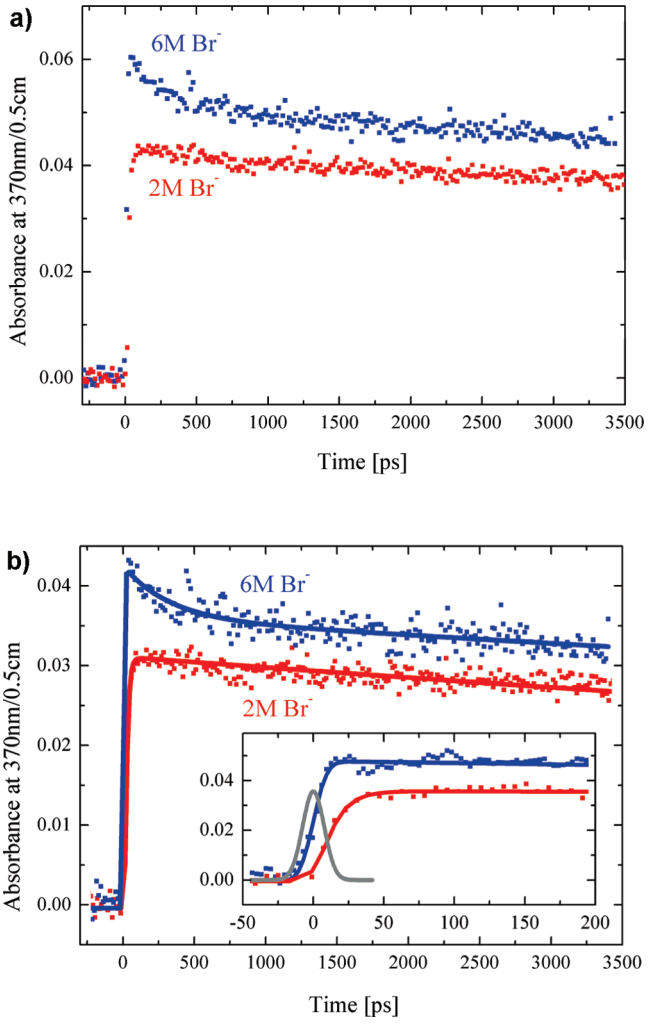

Figure 3. (a) Transient absorption of aqueous solutions of 2 and 6 M NaBr recorded from −300 ps to 3.5 ns at 370 nm. (b) Transient absorption of the product of oxidation of Br^- at 370 nm in aqueous solution of 2 and 6 M NaBr. The contribution of the solvated electron was subtracted from the raw data presented (a). Inset: same signals recorded on shorter time with a Gaussian presenting the apparatus function. The solid lines are drawn to guide the eye.

RESULTS

Five different types of aqueous halide solutions (Table 1) were examined at the picosecond electron pulse facility. First, the results obtained for the solutions containing Br^- ions are presented. The transient absorbance of a specific sample does not exhibit a significant change of shape or a shift after the electron pulse on the observed time scale.

Figure 1 shows the transient absorption spectra of 2 and 6 M NaBr and in pure water after the picosecond electron pulse. Besides the typical signature of the solvated electron with its large absorption band peaking at 718 nm, the transient spectra of the NaBr solutions reveal an additional band in the near UV that is attributed to the precursors of Br_3^-, that is, $BrOH^{-\bullet}$ and $Br_2^{-\bullet}$ radicals. The position and shape of the absorption spectra of the solvated electron are in agreement with the spectra obtained by nanosecond pulse radiolysis of Na^+ solutions.[30,31] The increase of the NaBr concentration causes an increase in the overall absorption amplitude and a shift of the absorption band of the solvated electron to shorter wavelengths. The data in this paper show that in spite of the increasing absorbance amplitude, the shape of the absorption band remains the same. Its maximum is blue-shifted by 12 and 27 nm for solutions containing 2 and 6 M Br^-, respectively. Such a spectral shift of the absorption band of the solvated electron in highly concentrated salt solutions was reported by several authors and is assigned to the electrostatic effect of the salt cations, here Na^+.[30−32] For the same irradiation conditions, the increase of absorbance above 500 nm for the highly concentrated Br^- solutions can be completely assigned to an increase of solvated electron concentration as no other species absorbs there. In fact, this increase must be due to the direct effect of radiation on the solute, that is, the ionization of Br^- forming $Br^\bullet$ and an electron that undergoes solvation on the femtosecond scale. Now, we will quantify this by analyzing the kinetics of the solvated electron. In Figure 2a, the decays in 2 and 6 M solutions of NaBr and in pure water are shown for a pulse probe delay from −30 ps to 3.5 ns at 575 nm. At this wavelength, only solvated electrons absorb. By increasing the Br^- concentration, the kinetics do not exhibit any change whereas the amplitude of the signal is increased directly from the time zero. At the molar concentrations of NaBr, the radiation is absorbed by water

dx.doi.org/10.1021/jp203609e |J. Phys. Chem. A 2011, 115, 9151–9159

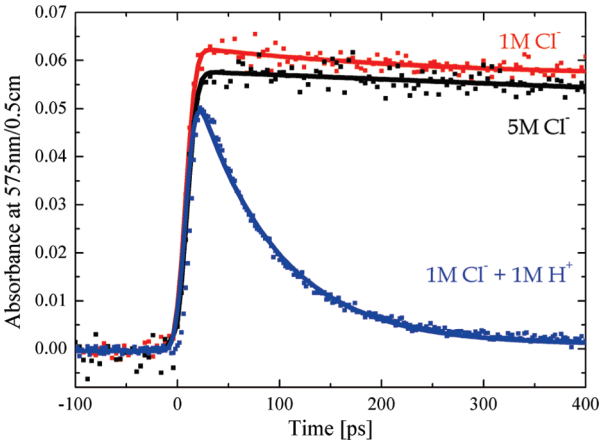

Figure 4. Solvated electron decay recorded at 575 nm in aqueous solutions of 1 and 5 M NaCl and 1 M NaCl with 1 M $HClO_4$ after normalization of the absorbed radiation dose (for details see text).

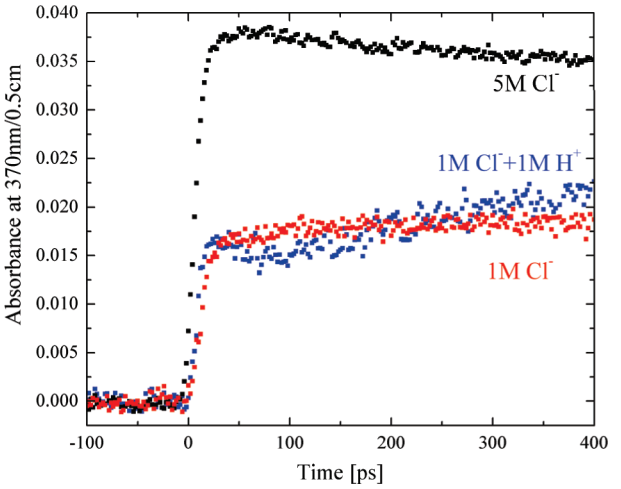

Figure 5. Transient absorption of aqueous solutions of 1 and 5 M NaCl and 1 M NaCl with 1 M $HClO_4$ recorded at 370 nm.

molecules and also by the solutes. To consider the dose additionally absorbed by the solute, the absorbed dose in pure water should be multiplied by the factor F:[17]

$$F = d_{sol}(Z_{NaBr}p/A_{NaBr} + Z_{water}(100-p)/A_{water})(Z_{water}100/A_{water})^{-1} \quad (1)$$

d_{sol} is the density of the solution, Z is the number of electrons, A is the mass number, and p is the weight fraction of the solute. The dose absorbed by the solution is:

$$D_{sol} = F \times D_{pure\ water} \quad (2)$$

The value of F is 1.1 and 1.29 for the solution containing 2 and 6 M Br^-, respectively (Table 1). The kinetics of the solvated electron decay measured in solutions 1 and 2 after this dose correction are shown in Figure 2b. Here, to obtain comparable amplitudes in regard to the concentration of the solvated electron, the above-mentioned blue shift of the absorption spectra that implies a difference of the extinction coefficient for 2 and 6 M solution at a given wavelength was taken into account. After the dose correction, the kinetics are found to be the same for both solutions and reveal identical amplitudes pointing clearly out that the increase of absorbance is due to the direct radiation effect on the solute.

For the same scans and therefore for identical experimental conditions, the kinetics of $BrOH^{-\bullet}$ and $Br_2^{-\bullet}$ formation are traced at 370 nm (Figure 3a). At this wavelength, apart from $BrOH^{-\bullet}$ and $Br_2^{-\bullet}$, the solvated electron contributes also to the absorbance. To investigate the absorbance at 370 nm revealing the $BrOH^{-\bullet}$ and $Br_2^{-\bullet}$ formation, the absorbed dose and the contribution of the solvated electron should be taken into account. To subtract the absorbance of the solvated electron, we considered once again the shift of its absorption band, depending on the concentration of NaBr. After these corrections, we obtain the kinetics at 370 nm presenting only the absorption of the oxidized Br^- species (Figure 3b). As we can observe, the kinetics at 370 nm are very different for these two solutions showing an important effect of the Br^- concentration. At 6 M, the change of the absorption is higher and a fast decay is present within the first 1000 ps. In contrast, for the 2 M solution, only a slow decay is observed within 4 ns. The difference between these two signals shows that the species formed after the electron pulse and absorbing at 370 nm are not the same.

Similar measurements were carried out in solutions containing 1 and 5 M Cl^- (Table 1). The picosecond studies of 1 and 5 M NaCl neutral aqueous solutions show (Figure 1, bottom) that the absorption spectrum of the solvated electron is blue-shifted relative to that of the pure water solution by 10 and 25 nm, respectively. The shape and shift of the transient absorption spectra is similar to the spectra recorded in aqueous solution of sodium bromide and remains time independent. Figure 4 shows the decays of the solvated electron for solutions 3, 4, and 5 observed at 575 nm after dose normalization and by taking into account the shift of absorption band, as we proceeded in the case of Br^- solutions. In acidic solution (sample 5), the solvated electron decays very fast by reacting with H^+. By fitting the decay kinetics, with considering the apparatus function and a single exponential function, the corresponding decay time is 79 ps. The corresponding value of the rate constant is 1.3×10^{10} M^{-1} s^{-1}. As we expected, due to the ionic strength effect this value is lower than that found in diluted solution (2.3×10^{10} M^{-1} s^{-1})[33] but it is very close to those already published for highly concentrated solutions.[8,33,34] After the corrections, the decay kinetics of the solvated electron as well as the amplitude of its absorption are very similar in solutions 3 and 4 without bearing whiteness of any effect of the Cl^- concentration. The species responsible for the absorption at 370 nm are presumably $Cl_2^{-\bullet}$ and $ClOH^{-\bullet}$ and in less extended part the solvated electron. Figure 5 reports the kinetics observed at 370 nm in solutions 3, 4, and 5, whereas Figure 6 shows the corresponding kinetics after dose normalization and subtraction of the solvated electron contribution. For neutral solutions, we found that the kinetics observed for the two different concentrations of Cl^- ions are strongly different. After correction (Figure 6), the initial amplitude of the signal for 5 M NaCl is 4 times higher compared to that of 1 M NaCl. The effect of Cl^- concentration on the kinetics observed in the UV is stronger than that reported above for Br^- solutions. In particular, we observe that the amplitude of the kinetics are very different compared to the case of Br^-. Moreover, for sample 3 (1 M Cl^-), the signal increases up to 1.5 ns, whereas for sample 4 (5 M Cl^-) the increase is very fast, on the range of the experimental time

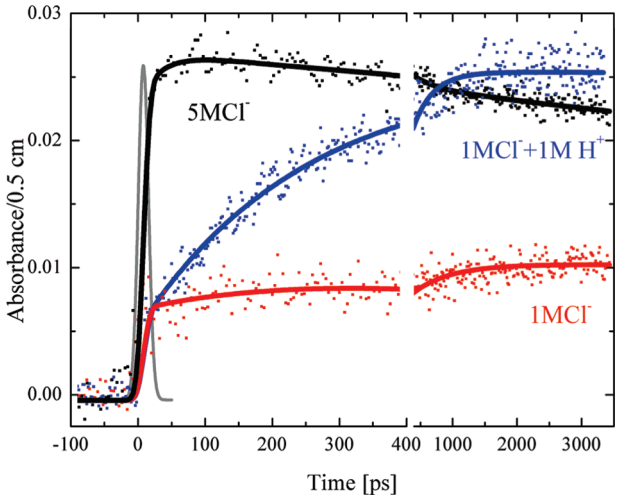

Figure 6. Transient absorption of the product of oxidation of Cl^- at 370 nm in an aqueous solution of 1 and 5 M NaCl and 1 M NaCl with 1 M $HClO_4$. The contribution of the solvated electron is subtracted from the raw data presented in Figure 5. The solid lines are drawn to guide the eye.

resolution and only a slow decay is observed. Transient absorption signals probed at 370 nm in solutions 3, 4, and 5 recorded from −100 ps to 3.5 ns are shown in Figure 6. For the solution containing 1 M H^+, the absorbance reaches its maximum around 2 ns after the electron pulse and does not change until 3.5 ns. A similar amplitude is observed almost directly after the pulse in the case of solution 4 containing 5 M NaCl.

DISCUSSION

The radiolytic oxidation of bromide ions, Br^-, in aqueous solution is well studied and involves several reactions. Rafi and Sutton[35] first demonstrated that the γ-radiolysis of aerated aqueous solutions of potassium bromide, KBr, in the concentration range 10^{-4} − 1 M generates bromine, Br_2, in equilibrium with the tribromide ion, Br_3^-. Pulse radiolysis studies by Rabani and co-workers[36−38] on deaerated KBr aqueous solutions established the mechanism and determined many of the rate constants. Later, D'Angelantonio et al.[39] re-examined the pulse radiolysis of Br^- aqueous solutions and determined other rate constants involved in this system. Recently, the rate constant of $Br_2^{-\bullet}$ decay was also reported at different temperatures.[40] In our case, the main difference is that the concentrations of the two studied solutions are very high and the measurements are performed on the picoseconds range. Considering the two kinetics of the solvated electron reported in Figure 2a, we did not observe any difference between them (except the amplitude) and we may conclude that there is no effect of Br^- concentration on the chemical process induced by radiation. It seems that the spur reactions are not affected in the presence of highly concentrated Br^- or Cl^-. All kinetics observed for solvated electrons are identical over 4 ns. In fact, the solvated electrons in these solutions are paired with Na^+ and usually the rate constant of a reaction between charged particles is much less affected at high ionic strength than at low ionic strength. We reported the rate constant of H^+ with the solvated electron in 0.2 M Cl^-[8] and we showed that the rate constant is slightly decreased compared to that of diluted solutions. Here the concentrations are even higher and we can expect a less effect on the rate constant of the solvated electron. Several models explain such behavior at very high ionic strength where the usual Debye equation is no more valid. In contrast, the signals reported in Figure 3b at 370 nm (without contribution of the solvated electron and after dose normalization) show an important difference between the kinetics of solutions 1 and 2. The difference suggests that the transient species formed on the picosecond range are not the same for the two solutions 1 and 2. Let us assume that for 6 M Br^- solution, the main species formed after the pulse is $Br_2^{-\bullet}$ and that for 2 M Br^- solution is $BrOH^{-\bullet}$. There are two observations to support this statement. For a given absorbed dose, the two main differences between the signals are that the amplitude for solution 2 is higher than for solution 1. Moreover, the decay within the first 1 ns observed for solution 2 is absent for solution 1. It is known that the extinction coefficient around the maximum (360 nm for both species) of $Br_2^{-\bullet}$ is higher than that of $BrOH^{-\bullet}$ ($\varepsilon_{BrOH^{-\bullet}}/\varepsilon_{Br_2^{-\bullet}} = 0.7$).[37] This explains the higher amplitude for signals of solution 2 observed at 370 nm. Second, it is known that each $Br_2^{-\bullet}$ can react very fast with another one to form Br_3^-, even in the spurs.[22] In our case, the fast decay of $Br_2^{-\bullet}$ can be attributed to the reactions in the spurs forming Br_3^- similar to the $OH^\bullet$ reaction in the spurs forming H_2O_2.

$$Br_2^{-\bullet} + Br_2^{-\bullet} \rightarrow Br_3^- + Br^- \quad (3)$$

The extinction coefficient of Br_3^- at this wavelength is only 740 M^{-1} cm^{-1}, that is, more than 15 times lower than those of $BrOH^{-\bullet}$ or $Br_2^{-\bullet}$. Then, reaction 3 leads to an absorption decay as experimentally observed. The rate constant of this reaction is 2.4×10^9 M^{-1} s^{-1}.[39] It could be faster in highly concentrated solution. The corresponding reaction between two $BrOH^{-\bullet}$ is not reported in the literature, and even if it could exist, the rate should be lower compared to the reaction with another Br^-. In fact, in the case of Cl^- solutions at neutral pH, for which $ClOH^{-\bullet}$ does not react with Cl^- on the picosecond time range, the reaction between two $ClOH^{-\bullet}$ is not observed. We can expect the same behavior for $BrOH^{-\bullet}$ which contrarily to $ClOH^{-\bullet}$ reacts with another Br^- to form $Br_2^{-\bullet}$. Reaction 3 explains why we do not observe a fast decay in the signal at 370 nm for the solution containing 2 M Br^-. These observations are in agreement with our statement that the main species absorbing at 370 nm are not the same after the picosecond electron pulse. Now, we have to justify this statement. First, it is worth noting that by assuming an additivity between direct and indirect effects of ionizing radiation, the radiolytic yield for a given transformation can be expressed by the following relation:

$$G = f_s G_s + (1 - f_s) G_w \quad (4)$$

where f_s is the ratio of the energy directly absorbed by the solute S (here Br^- or Cl^-) to the total energy absorbed by the solution. Energy loss of the electron beam due to the Compton effect is the major source of ionization in the medium and to a first approximation f_s can be evaluated by considering the electron fraction of the solute. G_s is the radiolytic yield due to the direct effect. G_w is the yield of the indirect effect and expresses the yield of the radiolytic species formed in water that participate in the oxidization of Br^-. Recently, we showed by γ-radiolysis of concentrated Br^- solutions the direct effect of ionizing radiation.[22] The direct ionization of the solute was shown to be not negligible for solutions with Br^- concentration greater than 2 M. When the concentration of Br^- is 6 M, 38% of the dose is absorbed by the solute (Table 1). The direct ionization of Br^- (directly or

dx.doi.org/10.1021/jp203609e |J. Phys. Chem. A 2011, 115, 9151–9159

through an excited state) can be considered as follows:

$$Br^- \rightarrow Br^\bullet + e^- \quad (5)$$

The $Br^\bullet$ radicals react very quickly with Br^- to form $Br_2^{-\bullet}$

$$Br^\bullet + Br^- \rightarrow Br_2^{-\bullet} \quad (6)$$

(1.2×10^{10} dm^3 mol^{-1} s^{-1} [41]).

According to reaction 6, when the concentration of Br^- is 6 M, this reaction ($t_{1/2}$ = ln 2/(6 mol dm^{-3} × 1.2×10^{10} dm^3 mol^{-1} s^{-1}) = 9.6 ps) occurs within the experimental time resolution of about 20 ps. But reaction 6 cannot explain solely the total fast formation of $Br_2^{-\bullet}$ observed within the electron pulse. If 38% of the absorbed dose acts directly on the solute, 62% of that interacts with the solvent molecules. When water is ionized, at first the $H_2O^{+\bullet}$ radical cation is formed by the electron pulse. But when the concentration of Br^- is 6 M, each water molecule has a Br^- ion just at contact. Then, we can consider the following reaction in the prethermal step:

$$Br^- + H_2O^{+\bullet} \rightarrow Br^\bullet + H_2O \quad (7)$$

The $H_2O^{+\bullet}$ radical is a highly oxidizing species, and at high concentration, reaction 7 replaces the reaction of the proton transfer between $H_2O^{+\bullet}$ and H_2O, which occurs usually within less than 100 fs in pure water. But, if the proton transfer is ultrafast in pure water (even a value of around 10 fs is reported for the proton transfer reaction[42,43]), for the solution containing 6 M Br^- (total 12 M cations and anions), this reaction can be avoided just by the absence of a water molecule close to the $H_2O^{+\bullet}$ cation. Each water molecule is related to a cation or an anion, therefore a direct charge transfer from Br^- to $H_2O^{+\bullet}$ could be proposed. Again $Br^\bullet$ formed through reaction 7 is converted within the pulse into $Br_2^{-\bullet}$. By this mechanism $OH^\bullet$ radicals are not formed and do not contribute to the oxidation of Br^-. Therefore, reactions 5−7 explain why at 6 M, $BrOH^{-\bullet}$ is almost not formed and the oxidation process forms mainly $Br_2^{-\bullet}$ just within the picosecond time resolution. In contrast, for 2 M solution (sample 1), reaction 6 is negligible because only less than 15% of the dose is absorbed by Br^- and the most important ionization is that of water molecules. Moreover, reaction 7 is also almost negligible because the concentration of Br^- is only 2 M and the main reaction of the $H_2O^{+\bullet}$ cation radical is that of fast proton transfer with another water molecule leading to the formation of the $OH^\bullet$ radical. Therefore, the main reaction with Br^- is the following:

$$OH^\bullet + Br^- \rightarrow BrOH^{-\bullet} \quad (8)$$

(1.1×10^{10} dm^3 $mol^{-1}s^{-1}$ [37]).

In this work, we assume that the product of reaction 8 does not depend on Br^- concentration. In fact, one could also speculate that when the hydroxyl is generated right in the coordination sphere of Br^-, the energetics could change and reaction 8 goes directly to $Br^\bullet$ and OH^-. Such a hypothesis is not considered here, and even for the sample containing 6 M Br^-, we consider that, if reaction 8 occurs, its product is only $BrOH^{-\bullet}$.

For sample 1 (2 M Br^-), $Br_2^{-\bullet}$ can only be formed at a longer time, within a few nanoseconds, through the following reaction:

$$BrOH^{\bullet-} + Br^- \rightarrow Br_2^{-\bullet} + OH^- \quad (9)$$

(1.9×10^8 dm^3 $mol^{-1}s^{-1}$ [37]).

For sample 1, we expect, therefore, the formation of $BrOH^{-\bullet}$ through reaction 8 within several tens of picoseconds ($t_{1/2}$ = ln 2/(2 mol dm^{-3} × 1.1 × 10^{10} dm^3 mol^{-1} s^{-1}) = 31 ps).

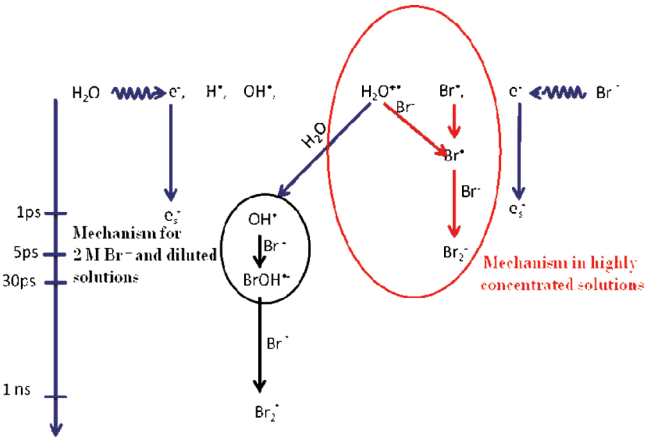

Figure 7. Scheme of the Br^- oxidation mechanism under ionizing radiation in highly concentrated sodium bromide aqueous solutions. The spur reactions, such as $Br_2^- + e_s^- \rightarrow 2Br^-$ and $2\ Br_2^- \rightarrow Br_3^- + Br^-$ are not represented on the scheme.

Kinetics scans on the short time scale, shown in the inset of Figure 3b, reveal clearly the discussed differences between two samples with 2 and 6 M Br^-. We fitted the data considering the time resolution of the setup as a Gaussian with fwhm = 18 ps (see Experimental Section) reported in Figure 3b. For 6 M Br^-, the absorption is formed within the apparatus function time, no exponential grow up was revealed by the fitting routine. In contrast, the built up of a significant absorption of the solution with 2 M Br^- is clearly delayed relative to the time zero. The formation time is distinctly longer than that of the apparatus function and that of 6 M Br^-. The maximum of absorption is reached only after 50 ps. We note that, in both cases (samples 1 and 2), the spur reactions between $Br_2^{-\bullet}$ and $BrOH^{-\bullet}$ with solvated electrons and $H^\bullet$ atoms occur. The slow decay observed at 370 nm is due to these reactions. That decay is also observed in the signals of the solvated electron (Figure 2a,b). In both cases, the solvated electron decays slowly with a rate identical within the precision of the measurement. But for sample 2, we have a supplementary spur reaction for $Br_2^{-\bullet}$ which forms Br_3^-. The scheme reported in Figure 7 resumes the mechanism of Br^- oxidation, showing how for 6 M Br^-, $Br_2^{-\bullet}$ is formed very rapidly.

In the case of Cl^- solutions, the same assumption can be done and it is more clear from our observations to confirm the statement that, for 5 M Cl^-, the main species formed after the picosecond electron pulse is $Cl_2^{-\bullet}$, and at 1 M, it is $ClOH^{-\bullet}$. There are three considerations supporting our assumption. First, at 370 nm the extinction coefficient of $ClOH^{-\bullet}$ is two times lower than that of $Cl_2^{-\bullet}$. The value of $\varepsilon_{\lambda=370\ nm}$ is 3500 and 7300 M^{-1} cm^{-1} for $ClOH^{-\bullet}$ and $Cl_2^{-\bullet}$, respectively.[44] Second, the decomposition of $ClOH^{-\bullet}$ is fast (reaction 11), and due to this reaction, in neutral solution not all $OH^\bullet$ radicals are converted to $ClOH^{-\bullet}$. We have then to consider the following equilibrium:

$$OH^\bullet + Cl^- \rightarrow ClOH^{-\bullet} \quad (10)$$

(4.3×10^9 L $mol^{-1}s^{-1}$ [44]).

$$ClOH^{-\bullet} \rightarrow Cl^- + OH^\bullet \quad (11)$$

(6.1×10^9 s^{-1} [44]).

Third, in acidic solution, it is possible to displace that equilibrium by converting all $OH^\bullet$ radicals to form $Cl_2^{-\bullet}$. Then,

$ClOH^{-\bullet}$ can be transformed totally into $Cl_2^{-\bullet}$ only in acidic medium through the following reactions:

$$ClOH^{-\bullet} + H^+ \rightarrow Cl^\bullet + H_2O \quad (12)$$

(2.1×10^{10} L mol^{-1}s^{-1} [44]).

$$Cl^\bullet + Cl^- \rightarrow Cl_2^{-\bullet} \quad (13)$$

(8.5×10^9 L mol^{-1}s^{-1} [45]).

We can explain the kinetics observed at 370 nm after dose normalization and subtraction of the solvated electron contribution (Figures 6b and 7) by considering these three observations. First, in neutral solution we observe an important difference between the absorbance amplitude of the sample 3 (1 M NaCl) and 4 (5 M NaCl). The initial signal for sample 4 is more than 4 times higher than that of sample 3. The difference can be understood by considering that for sample 4, $Cl_2^{-\bullet}$ is formed within the electron pulse by two processes: first, the direct ionization of Cl^-:

$$Cl^- \rightarrow Cl^\bullet + e^- \quad (14)$$

which is followed by a fast reaction 13 to form $Cl_2^{-\bullet}$, and second, by the oxidation of Cl^- with $H_2O^{+\bullet}$, as we reported above for Br^-:

$$Cl^- + H_2O^{\bullet+} \rightarrow Cl^\bullet + H2O \quad (15)$$

which is also followed by reaction 13. Therefore, for sample 4, the intense absorption observed just after the pulse is due to total conversion of the oxidation process to $Cl_2^{-\bullet}$, which presents a higher value of molar extinction coefficient than $ClOH^{-\bullet}$. According to reaction 13, the corresponding exponential formation time for a concentration of 5 M is 24 ps, that is, slightly larger than the time resolution of the setup. From the fit shown in Figure 6, we found a contribution with an exponential time constant of 30 ps. In fact, compared to the case of sample 2 (6 M Br^-), the concentration of Cl^- is lower (5 M) and the rate constant of $Cl_2^{-\bullet}$ formation is also slightly lower than that of reaction 6. Therefore, besides a fast total formation of Br_2^- (Figure 3b), we observe a slight increases of the absorbance shortly after the pulse (Figure 6). But when the concentration of Cl^- is lower (sample 3), the direct effect is almost negligible because less than 5% of the dose is absorbed by solutes (Table 1). Therefore, reaction 14 is unlikely. Moreover, the concentration of Cl^- is not high enough to favor reaction 15. Therefore, for the sample with 1 M Cl^-, the predominant species formed after the electron pulse is $ClOH^{-\bullet}$ resulting from reaction 10 in equilibrium with reaction 11. The molar extinction coefficient of $ClOH^{-\bullet}$ is two times lower than that of $Cl_2^{-\bullet}$. Moreover, the $ClOH^{-\bullet}$ radical is in equilibrium with $OH^\bullet$, with a fast back reaction. These considerations explain why the signals reported in Figure 6 are so different. For the same concentration (1 M) but in acidic pH (sample 5), the signal just after the electron pulse is similar to that of sample 3 (1 M), showing that only $ClOH^{-\bullet}$ is formed after the pulse. But at a longer time (around 4 ns) the amplitude of the signal for sample 5 reaches that of sample 4 (5 M), at short time showing that finally $Cl_2^{-\bullet}$ is formed through reactions 10, 12, and 13 in acidic medium. In fact, for sample 5, the direct effect (reaction14) is also negligible, but for that case, the low pH favors the formation of $Cl_2^{-\bullet}$ at longer times. Figure 8 resumes the mechanism of $Cl_2^{-\bullet}$ formation under ionizing radiation. We note that, in the case of Br^-, the formation of $Br_2^{-\bullet}$ is also favored in neutral solution at 2 M concentration through reaction 9. Such a reaction is not favored for neutral Cl^- solutions of 1 M concentration.

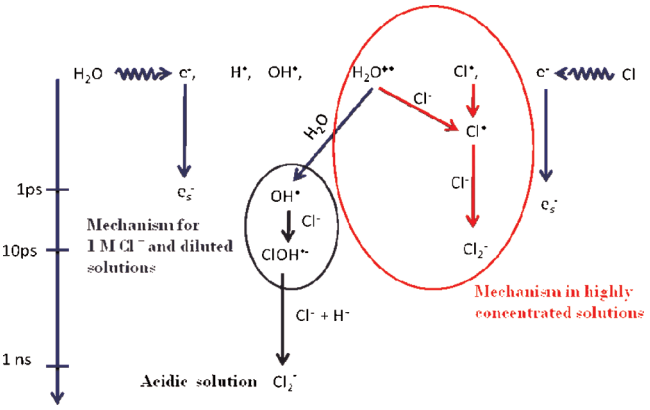

Figure 8. Scheme of the Cl^- oxidation mechanism in highly concentrated sodium chloride aqueous solutions. The spur reactions are not presented on the scheme.

In the rest of the discussion we try to examine three other possibilities to explain our results of Br^- and Cl^- oxidation. First of all, we know that due to the change of the refraction index of the solution the Cerenkov light is more intense in the highly concentrated halides solutions. The intensity of this light is much more important in the UV than in the visible, and it is known that Br^- and Cl^- anions absorb light in the UV. The extinction coefficient of the CTTS absorption band of Br^- and Cl^- changes with the concentration of Br^- and Cl^-, respectively.[10] At low concentration of Br^- and Cl^-, the maximum of the CTTS band is located at 208 and 193 nm with an extinction coefficient of around 300 and 500 M^{-1} cm^{-1}, respectively. Therefore, we can consider that the fast formation of $Br_2^{-\bullet}$ and $Cl_2^{-\bullet}$ could be due to the ionization of Br^- and Cl^- according to the following reaction which occurs during the pulse duration:

$$X^- + h\nu(\text{Cerenkov}) \rightarrow X^\bullet + e^- \quad (16)$$

X^- stands for the halide anion. For highly concentrated halide solutions, the halide atom then reacts rapidly with another X^- to form the dimer, $X_2^{-\bullet}$, almost within the electron pulse. However, if such a contribution (reaction 16) exists, the effect has also to be observed on the solvated electron signals. By ionization of halide anions with Cerenkov light, the absorbance of the solvated electron should increase markedly with increasing concentration of halide anions. But, in our case, for a given absorbed dose, almost the same amount of solvated electron is produced after the pulse. Therefore, we can exclude a measurable contribution of the Cerenkov light on the fast formation of the atom halide. We note that reaction 16 can occur also through an intermediate (for example, an excited state (X^{-*})); by considering such an intermediate, the discussion above concerning the balance does not change in any case.

The second possible reaction path considers the ionization of halide anions by the excited state of a water molecule:

$$X^- + H_2O^* \rightarrow X^\bullet + H_2O + e^- \quad (17)$$

Such a reaction or a similar reaction with an intermediate excited state X^{-*} could be possible. But, as we reported above, reaction 17 should also change the absorbance of the solvated electron produced by solvation of the ejected electron. Therefore, reaction 17 is not responsible for the important amount of $Br_2^{-\bullet}$ and $Cl_2^{-\bullet}$ formed within the electron pulse for 6 and 5 M Br^- and Cl^- solution, respectively.

Finally, the last possibility that we have to consider is the effect of ionic strength. The formation of Br_2^- and Cl_2^- at the end of the pulse could be ascribed to the following reaction:

$$X_2^{2-} + OH^\bullet \rightarrow X_2^{\bullet -} + OH^- \quad (18)$$

In fact, it was reported that halide anion pairs, X_2^{2-}, are formed at high concentration in aqueous solutions.[46] Reaction 18 is an alternative to the reaction between X^- and $H_2O^{+\bullet}$ to explain the fast formation of $X_2^{-\bullet}$ after the picosecond electron pulse. In that case, $OH^\bullet$ radical remains the source of $X_2^{-\bullet}$ formation, as in diluted solution, but reacting with a pair of two Cl^- (or Br^-) anions. However, more recent studies show that such a pair even at 5 M NaCl does not exist, and the $Cl^- - Cl^-$ pairing was an artifact of computations.[47] Therefore, the only reaction which could explain the fast formation of $X_2^{-\bullet}$ is the reaction of the halide anion with $H_2O^{+\bullet}$. Moreover, we did not observe a noticeable effect on the decay of solvated electron compared to that in pure water and all kinetics observed for solvated electrons are identical over 4 ns. That reveals that replacing $OH^\bullet$ radical by $Br_2^{-\bullet}$ or $Cl_2^{-\bullet}$ does not affect significantly the spur kinetics.

CONCLUSION

The picosecond electron-pulse supercontinuum-probe absorption setup is a powerful tool for the study of the reactions in highly concentrated solutions. A broadband probe pulse and a multichannel detection system were used to record the absorbance change of the halide species in the UV and of the solvated electron in the visible under identical conditions. This allowed us to separate and to analyze quantitatively the kinetics of the involved species. The present work confirms our conclusions on the direct ionization effect for the highly concentrated halide solutions. The analysis of the pulse-probe measurements on the picosecond range show that in the highly concentrated halide solutions, $Br_2^{-\bullet}$ and $Cl_2^{-\bullet}$ are formed within the electron pulse without formation of $BrOH^{-\bullet}$ and $ClOH^{-\bullet}$. The interesting result is that not only Br^- and Cl^- are directly ionized by the electron pulse, but that they also undergo prompt oxidation by water-related intermediates, possibly involving a hole in the coordination sphere of the hydrated halide anions. For more detailed descriptions of the spurs reactions on the picosecond range, and to verify a possible charge transfer from the precursor of $OH^\bullet$ radicals to the halide anions, it is necessary to include the presented results for the direct ionization effect in the usual simulation codes used in radiation chemistry and to find the parameters of such a reaction.

AUTHOR INFORMATION

Corresponding Author

*E-mail: mehran.mostafavi@u-psud.fr.

ACKNOWLEDGMENT

The ELYSE team thanks warmly RTRA Triangle de la Physique (Orsay, France) for financial support to renew the femtosecond laser of ELYSE facility.

REFERENCES

(1) Spotheim-Maurizot, M.; Mostafavi, M.; Douki, T.; Belloni, J. *Radiation Chemistry: From Basics to Applications in Material and Life Science*; EDP Sciences: France, 2008.

(2) Hatano, Y.; Katsumura, Y.; Mouzumder, A. *Charged Particle and Photon Interactions with Matter: Recent Advances, Applications and Interfaces*; CRC Press: New York, 2011.

(3) Dewaele, V.; Lampre, I.; Mostafavi, M. In *Charged Particle and Photon Interactions with Matter: Recent Advances, Applications and Interfaces*; Hatano, Y., Katsumura, Y., Mouzumder, A., Eds.; CRC Press: New York, 2011; pp 289−324.

(4) Buxton, G. V. In *The Radiation Chemistry of Liquid Water: Principles and Applications*; Mozumder, A., Hatano, Y., Eds.; Marcel Dekker: New York, 2004; pp 331−363.

(5) Bartels, D. M.; Gosztola, D.; Jonah, C. D. *J. Phys. Chem. A* **2001**, *105*, 8069–8072.

(6) Muroya, Y.; Lin, M.; Wu, G.; Iijima, H.; Yoshi, K.; Ueda, T.; Kudo, H.; Katsumura, Y. *Radiat. Phys. Chem.* **2005**, *72*, 169–172.

(7) Schuler, R. H.; Hartzell, A. L.; Behar, B. *J. Phys. Chem.* **1981**, *85*, 192–199.

(8) Atinault, E.; De Waele, V.; Schmidhammer, U.; Fattahi, M.; Mostafavi, M. *Chem. Phys. Lett.* **2008**, *460*, 461–465.

(9) Katsumura, Y. In *Radiation Chemistry: Present Status and Future Trends (Studies in Physical and Theoretical Chemistry)*; Jonah, C. D., Rao, B. S. M., Eds.; Elsevier: New York, 2001; Vol. 87, pp 163−174.

(10) Sauer, M. C., Jr; Shkrob, I. A.; Lian, R.; Crowell, R. A.; Bartels, D. M.; Chen, Xiyi; Suffern, D.; Bradforth, S. E. *J. Phys. Chem. A* **2004**, *108*, 10414.

(11) Matthews, R. W; Mahlman, H. A.; Sworski, T. J. *J. Phys. Chem.* **1972**, *76*, 2680.

(12) Daniels, M. *J. Phys. Chem.* **1969**, *73*, 3710.

(13) Kozlowska-Milner, E.; Broszkiewicz, R. K. *Radiat. Phys. Chem.* **1978**, *11*, 253.

(14) Pikaev, A. K.; Glazunov, P. Ya.; Yakubovich, A. A. *Dikl. Akad. Nauk SSSR* **1974**, *215*, 645.

(15) Lesigne, B.; Ferradini, C.; Pucheault, J. *J. Phys. Chem.* **1973**, *17*, 2156–2158.

(16) Katsumura, Y; Jiang, P. Y.; Nagaishi, R.; Oishi, T.; Ishigure, K.; Yoshida, Y. *J. Phys. Chem.* **1991**, *95*, 4435–4439.

(17) Pucheault, J.; Ferradini, C.; Julien, R.; Deysine, A.; Gilles, L.; Moreau, M. *J. Phys. Chem.* **1978**, *83*, 330–336.

(18) Hadjadj, A.; Julien, R.; Pucheault, J.; Ferradini, C.; Hickel, B. *J. Phys. Chem.* **1982**, *86*, 4630–4634.

(19) Woods, R. J.; Lesigne, B.; Gilles, L.; Ferradini, C.; Pucheault, J. *J. Phys. Chem.* **1975**, *79*, 2700–2704.

(20) Grigor'eva, A. E.; Makarov, I. E.; Pikaev, A. K. *High Energy Chem.* **1991**, *25*, 172.

(21) Mirdamadi-Esfahani, M.; Lampre, I.; Marignier, J. -L.; De Waele, V.; Mostafavi, M. *Radiat. Phys. Chem.* **2009**, *78*, 106–111.

(22) Balcerzyk, A.; LaVerne, J.; Mostafavi, M. *J. Phys. Chem. A* **2011**.

(23) Belloni, J.; Monard, H.; Gobert, F.; Larbre, J.-P.; Demarque, A.; De Waele, V.; Lampre, I.; Marignier, J. -L.; Mostafavi, M.; Bourdon, J. C.; Bernard, M.; Borie, H.; Garvey, T.; Jacquemard, B.; Leblond, B.; Lepercq, P.; Omeich, M.; Roch, M.; Rodier, J.; Roux, R. *Nucl. Instrum. Methods Phys. Res., Sect. A* **2005**, *539*, 527–539.

(24) Marignier, J. L.; De Waele, V.; Monard, H.; Gobert, F.; Larbre, J.-P.; Demarque, A.; Mostafavi, M.; Belloni, J. *Radiat. Phys. Chem.* **2006**, *75*, 1024–1033.

(25) Schmidhammer, U.; De Waele, V.; Marquès, J.-R.; Bourgeois, N.; Mostafavi, M. *Appl. Phys. B: Lasers Opt.* **2009**, *94*, 95–101.

(26) De Waele, V.; Schmidhammer, U.; Marquès, J.-R.; Monard, H.; Larbre, J.-P.; Bourgeois, N.; Mostafavi, M. *Radiat. Phys. Chem.* **2009**, *78*, 1099–1101.

(27) Belloni, J. ; Crowell, R. A.; Katsumura, Y.; Lin, M.; Marignier, J.-L.; Mostafavi, M.; Muroya,Y.; Akinori, S.; Tagawa, S.; Yoshida, Y. De Waele, V.; Wishart, J. F. In *Recent Trends in Radiation Chemistry*; Wishart, J. F., Rao, B. S. M, Eds.; World Scientific: NJ, 2010; pp 121−160.

(28) De Waele, V.; Sorgues, S.; Pernot, P.; Marignier, J.-L.; Monard, H.; Larbre, J.-P.; Mostafavi, M. *Chem. Phys. Lett.* **2006**, *423*, 30–34.

(29) Schmidhammer, U.; Pernot, P.; De Waele, V.; Jeunesse, P.; Demarque, A.; Murata, S.; Mostafavi, M. *J. Phys. Chem. A* **2010**, *114*, 12042–12051.

(30) Wolff, R. K.; Aldrich, J. E.; Penner, T. L.; Hunt, J. W. *J. Phys. Chem.* **1975**, *79* (3), 210–219.
(31) Anbar, M.; Hart, E. J. *J. Phys. Chem.* **1965**, *69* (4), 1244.
(32) Bonin, J.; Lampre, I.; Mostafavi, M. *Radiat. Phys. Chem.* **2005**, *74*, 288–296.
(33) Jonah, C. D.; Miller, J. R.; Matheson, M. S. *J. Phys. Chem.* **1977**, *81*, 931–934.
(34) Bronskill, M. J.; Wolff, R. K.; Hunt, J. W. *J. Chem. Phys.* **1970**, *53*, 4201.
(35) Rafi, A.; Sutton, H. C. *Trans. Faraday Soc.* **1965**, *61* (509), 877–890.
(36) Matheson, M. S.; Mulac, W. A.; Weeks, J. L.; Rabani, J. *J. Phys. Chem.* **1966**, *70*, 2092–2099.
(37) Zehavi, D; Rabani, J. *J. Phys. Chem.* **1972**, *76*, 312–319.
(38) Mamou, A.; Rabani, J.; Behar, D. *J. Phys. Chem.* **1977**, *81*, 1447–1448.
(39) D'angelantonio, M.; Venturi, M.; Mulazzani, Q. G. *Radiat. Phys. Chem.* **1988**, *32*, 319–324.
(40) Lin, M.; Archirel, P.; Van-Oanh, N.; Muroya, Y.; Fu, H.; Yan, Y.; Nagaishi, R.; Kumagai, Y.; Katsumura, Y., Mostafavi; M. *J. Phys. Chem. A* **2011**.
(41) Merenyi, G.; Lind, J. *J. Am. Chem. Soc.* **1994**, *116*, 7872–7876.
(42) De Waele, V.; Lampre, I.; Mostafavi, M. In *Charged Particle and Photon Interactions with Matter*; Hatano, Y., Katsumura, Y., Mozumder, A., Eds.; CRC Press: New York, 2011; pp 289−324.
(43) Garrett, B. C.; Dixon, D. A.; Camaioni, D. M.; Chipman, D. M.; Johnson, M. A.; Jonah, C. D.; Kimmel, G. A.; Miller, J. H.; Rescigno, T. N.; Rossky, P. J.; Xantheas, S. S.; Colson, S. D.; Laufer, A. H.; Ray, D.; Barbara, P. F.; Bartels, D. M.; Becker, K. H.; Bowen, H.; Bradforth, S. E.; Carmichael, I.; Coe, J. V.; Corrales, L. R.; Cowin, J. P.; Dupuis, M.; Eisenthal, K. B.; Franz, J. A.; Gutowski, M. S.; Jordan, K. D.; Kay, B. D.; LaVerne, J. A.; Lymar, S. V.; Madey, T. E.; McCurdy, C. W.; Meisel, D.; Mukamel, S.; Nilsson, A. R.; Orlando, T. M.; Petrik, N. G.; Pimblott, S. M.; Rustad, J. R.; Schenter, G. K.; Singer, S. J.; Tokmakoff, A.; Wang, L. S.; Wittig, C.; Zwier, T. S. *Chem. Rev.* **2005**, *105*, 355.
(44) Jayson, G. G.; Parsons, B. J.; Swallow, A. J. *J. Chem. Soc., Faraday Trans.* **1973**, *69* (1), 1597–1607.
(45) Buxton, G. V.; Bydeer, M.; Salmon, G. A. *J. Chem. Soc., Faraday Trans.* **1998**, *94* (5), 653–657.
(46) Dang, L. X.; Pettitt, B. M. *J. Phys. Chem.* **1990**, *94*, 4303.
(47) Hummer, G.; Soumpasis, D. M.; Neumann, M. *Mol. Phys.* **1993**, *81*, 1155.